


# A Rare Case of Papillary Thyroid Carcinoma in Marine-Lehnhart Syndrome—Indication for Biopsy of Hot Thyroid Nodules?

Jimmy Masjkur,<sup>1,2</sup>  Martin Thurnheer,<sup>1</sup> Ole Christopher Maas,<sup>3</sup> Roland Schuler,<sup>4</sup> and Christopher Strey<sup>1</sup>

<sup>1</sup>eSwiss Medical and Surgical Center, Klinik Stephanshorn, St.Gallen 9000, Switzerland

<sup>2</sup>Faculty of Medicine, Hasanuddin University, Makassar 90145, Indonesia

<sup>3</sup>Klinik für Radiologie und Nuklearmedizin, Kantonsspital St.Gallen, St.Gallen 9000, Switzerland

<sup>4</sup>PATHOdiagnostics AG, St.Gallen 9000, Switzerland

**Correspondence:** Jimmy Masjkur, Dr.med, MSc, eSwiss Medical and Surgical Center, Klinik Stephanshorn, Brauerstrasse 97, 9016 St.Gallen, Switzerland.  
Email: [jimmy.masjkur@eswiss.center](mailto:jimmy.masjkur@eswiss.center).

## Abstract

An uncommon occurrence in which Graves disease (GD) coincides with autonomous functioning thyroid nodules (AFTNs) is termed Marine-Lehnhart syndrome (MLS). While hyperfunctioning nodules in MLS are commonly benign, there exists a rare potential for malignancy. A 41-year-old male patient was initially managed conservatively upon being diagnosed with MLS type 1. However, the emergence of obstructive symptoms prompted a thyroidectomy 4 years after initial presentation. Histological analysis revealed 2 cervical lymph node metastases and papillary thyroid cancer (PTC) within the AFTN.

**Key Words:** thyroid cancer, hot nodule biopsy

**Abbreviations:** AFTN, autonomous functioning thyroid nodule; FNA, fine needle aspiration; GD, Graves disease; MLS, Marine-Lehnhart syndrome; PTC, papillary thyroid cancer; RAI, radioactive iodine; TSH, thyrotropin (thyroid-stimulating hormone).

## Introduction

Marine-Lehnhart syndrome (MLS) represents a rare manifestation of primary hyperthyroidism, marked by the concurrent presence of Graves disease (GD) and autonomously functioning thyroid nodules (AFTNs). While thyroid nodules are identified in 23% to 30% of GD patients, only a minority of these nodules exhibit autonomous functionality. The release of thyroid hormones from AFTN tissue can be intensified by thyrotropin (thyroid-stimulating hormone [TSH])-receptor stimulation facilitated by autoantibodies, a shared factor in both conditions. Genetic mutations in TSH receptors have been implicated in the pathogenesis of MLS (1-4). MLS is categorized into 3 subtypes according to scintigraphy patterns: type 1, characterized by a high-uptake thyroid gland with a single AFTN, as observed in our case; type 2, distinguished by a high-uptake thyroid with multiple AFTNs; and type 3, identified by the presence of additional cold nodules (5, 6).

Although hyperfunctioning nodules in MLS are generally benign, isolated cases of malignancy have been reported (7, 8). In this report, we present the case of a 41-year-old male patient diagnosed with MLS type 1, concomitant with papillary thyroid cancer (PTC).

## Case Presentation

A 41-year-old male individual was referred for assessment due to severe thyrotoxicosis. His medical history revealed hypertension, obesity, and a history of nicotine use, with no reported family history of thyroid disease.

## Diagnostic Assessment

Upon physical examination, a blood pressure of 175/95 mmHg and a pulse rate of 95 beats per minute were noted, with no indications of Graves ophthalmopathy or pretibial myxedema. The thyroid gland appeared enlarged and non-tender, with no discernible nodules upon palpation. Laboratory evaluation revealed a suppressed TSH level of <0.001 mIU/L (<0.001 IU/L) (normal reference range: 0.3-0.5 mIU/L [0.3-5 IU/L]), along with elevated levels of free thyroxine (FT4) at 34.19 pg/mL (44 pmol/L) (normal reference range: 8.54-20.19 pg/mL [11-26 pmol/L]) and free triiodothyronine (FT3) at 8.07 pg/mL (12.4 pmol/L) (normal reference range: 2.02-4.68 pg/mL [3.1-7.2 pmol/L]). TSH receptor antibodies (TRAb) were elevated at 10.1 mIU/L (10.1 IU/L) (normal reference range: <1.6 mIU/L [<1.6 IU/L]) (Table 1).

**Table 1. The validation of type 1 Marine-Lehnhart syndrome**

Hormone and antibody tested	First visit	Follow-up		Normal range
		Presurgery	Postsurgery	
TSH	< <b>0.001 mIU/L</b> (< <b>0.001 IU/L</b> )	2.3 mIU/L (2.3 IU/L)	9.7 mIU/L (9.7 IU/L)	0.3-5 mIU/L (0.3-5 IU/L)
Free thyroxine	<b>34.18 pg/mL</b> ( <b>44 pmol/L</b> )	10 pg/mL (12.9 pmol/L)	3.4 pg/mL (17.3 pmol/L)	8.5-17.8 pg/mL (11-23 pmol/L)
Free triiodothyronine	<b>8.07 pg/mL</b> ( <b>12.4 pmol/L</b> )	2.5 pg/mL (3.9 pmol/L)	2.3 pg/mL (3.5 pmol/L)	2-4.7 pg/mL (3.1-7.2 pmol/L)
TRAb	<b>10.1 mIU/L</b> ( <b>10 IU/L</b> )			< 1.6 mIU/L (< 1.6 IU/L)
TgAb	11.9 mIU/mL (11.9 IU/mL)			< 115 mIU/mL (11.9 IU/mL)
TPOAb	< 9 mIU/mL (< 9 IU/mL)			< 34 mIU/mL (< 34 IU/mL)
Thyroglobulin	<b>130 ng/mL</b> ( <b>130 µg/L</b> )			3.1-7.7 ng/mL (3.1-7.7 µg/L)

Pre- and postoperative plasma hormone and antibody concentrations in our patient.

Abnormal values are shown in bold font. Values in parenthesis are International System of Units (SI).

Conversion factors: free thyroxine, 1 pg/mL = 1.287 pmol/L; free triiodothyronine, 1 pg/mL = 1.5361 pmol/L.

Graves disease was confirmed through laboratory tests demonstrating elevated levels of TRAb, along with suppressed TSH, and elevated levels of FT4 and FT3.

Abbreviations: FT3, free triiodothyronine; FT4, free thyroxine; TgAb, thyroglobulin antibody; TPOAb, thyroid peroxidase antibody; TRAb, TSH receptors autoantibodies; TSH, thyroid-stimulating hormone.

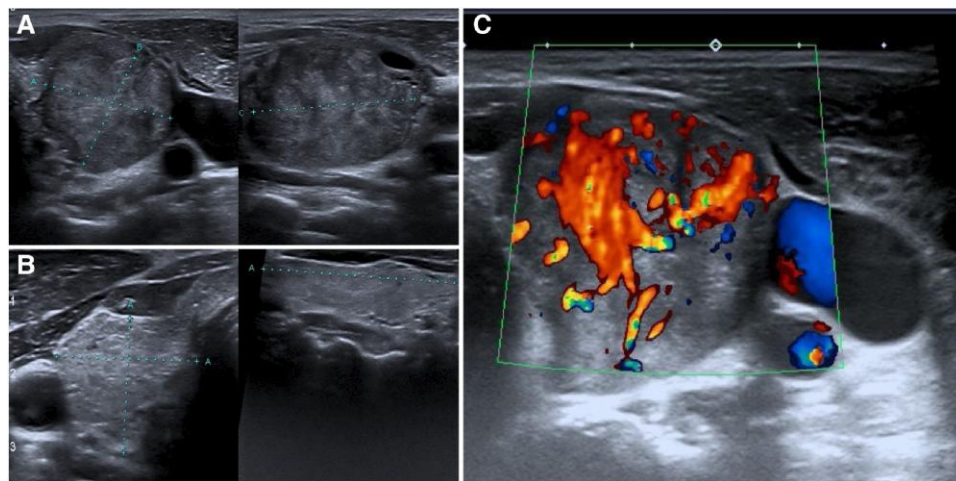


**Figure 1.** Ultrasonographic features of the hypervascular nodule. Thyroid ultrasonography depicted a highly vascularized nodule with a volume of 13 mL (A) and (C), in contrast to the contralateral side (B).

Ultrasonography depicted an enlarged thyroid with a total volume measuring 42 mL. Within this, the left lobe appeared predominantly replaced by a 27 × 24 × 33 mm heterogenous, isoechogenic, and notably vascularized nodule exhibiting a thin halo, devoid of any calcifications (Fig. 1). This nodule was categorized as TIRADS 3 (9, 10). A technetium-99m-perchnetate scintigraphy revealed not only a significantly increased uptake (3.11%) within the sonographically identified nodule but also diffusely elevated uptake throughout the entire thyroid gland (Fig. 2).

## Treatment

The patient was initiated on carbimazole treatment. Upon achieving biochemical and clinical remission, he elected against treatment discontinuation or definitive therapy. However, 4 years later, he presented with gradually worsening obstructive symptoms. Subsequent ultrasonography revealed an increase in the size of the nodule to 33 × 36 × 48 mm. Subsequently, a total thyroidectomy was performed without complications, followed by the initiation of thyroxine replacement therapy.

## Outcome and Follow-Up

The histological analysis of the 45 × 35 × 28 mm tumor exhibited discernible nuclear attributes consistent with PTC, notably characterized by central clearing, grooves, and enlarged size (Fig. 3). Noteworthy is the absence of any indication of extrathyroidal invasion. Furthermore, a cluster of neoplastic cells was identified proximate to the resection margin. The pathological staging of the tumor is delineated as follows: pT3a, pNX, L0 (invasion of lymphatic vessels), V0 (vein invasion), Pn0 (invasion of adjacent nerves), and R1 (signifying incomplete resection, denoting the presence of cancer cells at resection margins). A stimulated I-131-scintigraphy scan with single-photon emission computed tomography/computed tomography (SPECT/CT) conducted 5 weeks after thyroidectomy disclosed the presence of 2 lymph node metastases, each measuring 0.8 cm, localized at levels II and III (Fig. 4). During a multidisciplinary case conference, the consensus favored radioiodine therapy over operative neck dissection. Subsequently, 3 sessions of radioactive iodine treatments were administered over the span of a year, comprising doses of

3000, 7400, and 7400 MBq (or 81.08, 200, and 200 mCi, respectively). These treatments were prompted by the persistence of signals from 2 lymph nodes detected during follow-up evaluations (Fig. 4). At the conclusion of the second treatment regimen, faint signals were still discernible in the 2 affected lymph nodes. After TSH stimulation, thyroglobulin levels surged to 11.9 ng/mL (11.9 µg/L), following a significant decline to 2.0 ng/mL (2.0 µg/L) (normal reference range: <0.5 ng/mL [ $<0.5$  µg/L]). Subsequent to this observation,

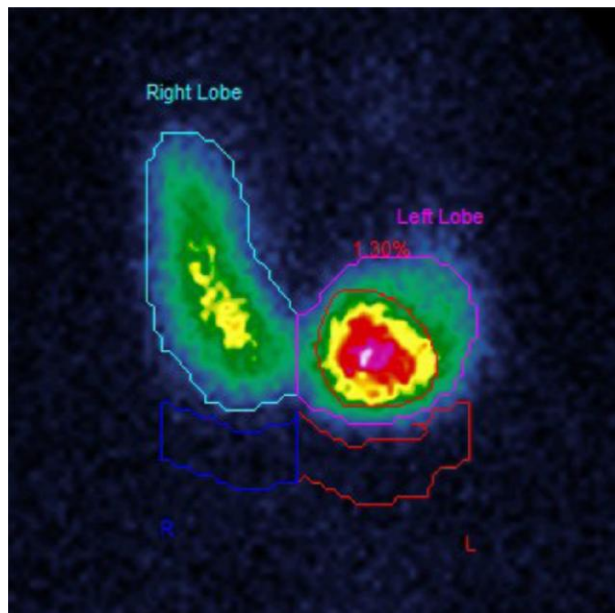


**Figure 2.** Scintigraphy scan illustrating an autonomous functioning thyroid nodule. The scintigraphy scan indicated a solitary intensely radiating hot nodule with a technetium uptake of 3.11%, situated at the lower pole of the left thyroid lobe.

further imaging studies were scheduled as part of the ongoing medical management.

## Discussion

The confirmation of MLS type 1 diagnosis was established through the presence of TRAb and scintigraphic evidence demonstrating an AFTN within a diffusely high-uptake thyroid gland. The unexpected identification of PTC underscored a potentially compromised prognosis attributed to delayed diagnosis. This case prompts consideration regarding the necessity of an initial fine needle aspiration (FNA) for diagnostic clarification.

Intranodular carcinoma within hyperfunctioning thyroid nodules represents a rare occurrence, posing challenges to preoperative diagnosis (11-13). Present guidelines advise against biopsies of hyperfunctioning nodules unless there is substantial suspicion of malignancy (5, 14).

Research indicates that patients with GD may exhibit a propensity for more aggressive forms of thyroid cancer, characterized by earlier lymph node and distant metastases in comparison to euthyroid controls (15). Our decision to refrain from preoperative FNA was predicated on the benign sonographic appearance (TIRADS 3) of the nodule, notwithstanding its substantial growth. However, it is noteworthy that even rapid growth of thyroid nodules does not reliably predict false-negative FNA cytology (16). The correlation between hot nodules and thyroid cancer has been subject to investigation (17). However, there remains a paucity of understanding regarding the concurrent occurrence of thyroid cancer with MLS. Scant reports exist in the literature, particularly in adult populations, and none have been documented in pediatric cohorts. Notably, in most documented instances, including our case, histopathological examinations have revealed PTC. Molecular sequencing analysis unveiled a singular instance of a BRAF V600E gene mutation. It is noteworthy that mutations in Rat sarcoma (RAS) and BRAF, as well as rearrangements in

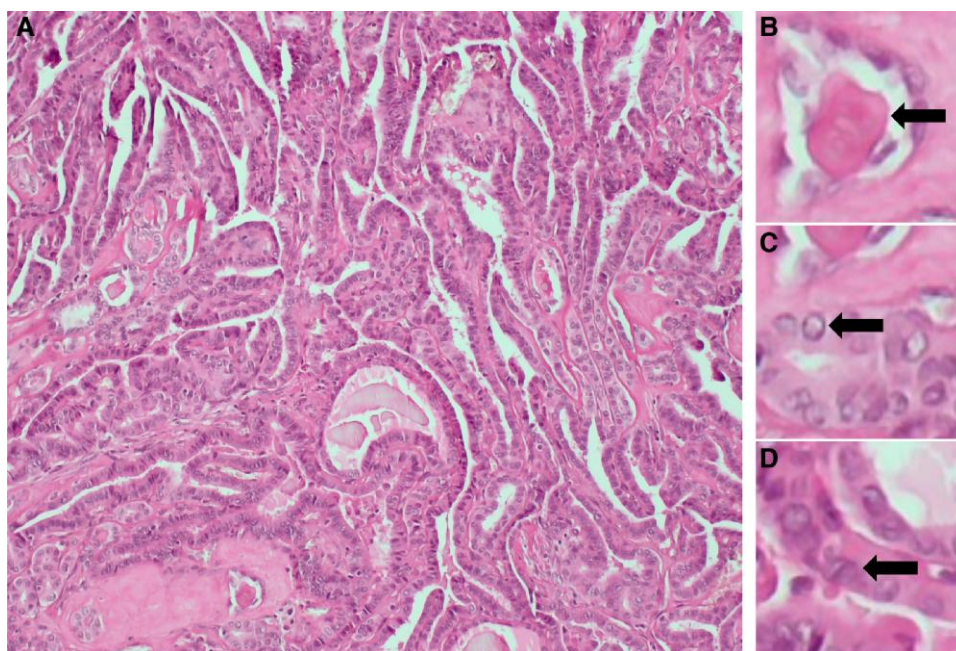


**Figure 3.** Classic variant of papillary thyroid carcinoma. The typical histological characteristics of papillary thyroid carcinoma encompass the presence of (A) psammoma bodies (B), papillary structures, as well as (C) distinctive nuclear features including central clearing and (D) grooves.



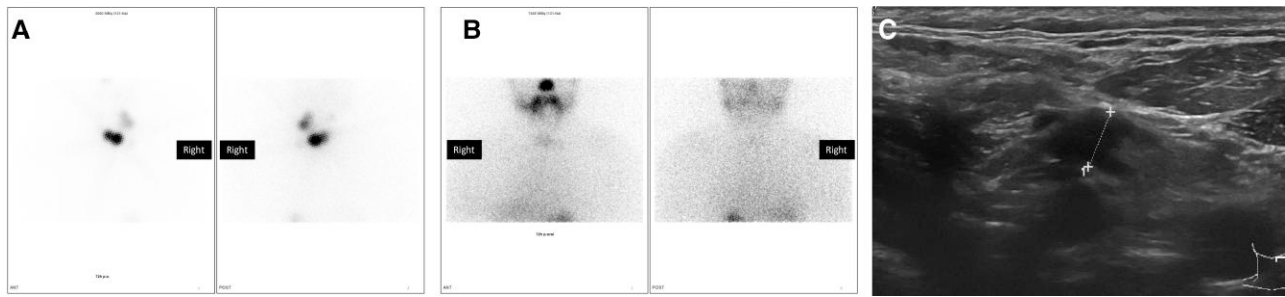


**Figure 4.** Detection of cervical lymph node metastases and subsequent remission following radioiodine ablation therapy. Postoperative scintigraphy revealed 2 iodine-avid cervical lymph nodes, measuring 0.8 cm each, positioned at levels II and III of the left lobe (A). A follow-up scan conducted 2 months after radioiodine ablation (RAI) exhibited notable nonspecific tracer accumulation in the respiratory tract mucous membranes, with minimal evidence of iodine-avid lymph nodes (B). Subsequent ultrasonography confirmed a faint persistent signal in these lymph nodes (C).

Paired-box (PAX) 8/Peroxisome proliferator-activated receptor gamma gene (PPARG) or Rearranged during transfection (RET)/PTC genes, have been discernible in a significant proportion of adult PTC cases but have been notably absent in pediatric populations. While reports of distant metastases are lacking, regional neck metastases were indeed detected in our patient (18-22). The necessity for a thyroid biopsy in an adult patient presenting with a hyperfunctioning nodule could be ascertained through genetic testing. In our case, the presence of lymph node metastases was initially overlooked during the initial exploration, primarily due to complete cavitation resulting from cystic degeneration, which mimicked the appearance of an ostensibly benign cervical cyst. Radioactive iodine (RAI) therapy may be contemplated in this scenario as an adjuvant measure, although it is typically not recommended following a hemithyroidectomy. Evidence from randomized trials has shown that radioiodine treatment was unnecessary in low-risk patients with differentiated carcinoma who had undergone thyroidectomy. Our patient exhibited a favorable response to RAI therapy, although its effectiveness in treating MLS patients remains a topic of debate (22-25). A fine needle biopsy could have facilitated the early detection of malignancy in this rare instance of a PTC found within the hyperfunctioning nodule of a patient with MLS type 1, thereby potentially improving the prognosis. To prevent overdiagnosis, the decision to perform a FNA on a hyperfunctioning nodule should be based on robust clinical evidence.

### Learning Points

- This case demonstrates the importance of contemplating a fine needle aspiration in instances of suspicious hyperfunctioning thyroid nodules manifesting high-risk features on ultrasonography and exhibiting rapid growth.
- Marine-Lehnhart syndrome should be incorporated into the list of differential diagnoses for Graves disease accompanied by coexisting nodules.
- It is essential to conduct a thorough clinical assessment in patients with Graves disease to exclude autonomously functioning thyroid nodules and thereby avoid unnecessary long-term thyrostatic medication.

### Contributors

All authors made individual contributions to authorship. J.M., M.T., O.C.M., and C.S. were involved in the diagnosis and management of the patient and manuscript submission.

R.S. was involved in histopathology section and preparation of histology images. M.T. was responsible for the patient's surgeries. All authors reviewed and approved the final draft.

### Funding

No public or commercial funding

### Disclosures

The authors declare that they have no financial relationships that could be broadly relevant to the work.

### Informed Patient Consent for Publication

Signed informed consent was obtained directly from the patient.

### Data Availability Statement

Original data generated and analyzed during this study are included in this published article.

### References

1. Fu H, Cheng L, Jin Y, Chen L. Thyrotoxicosis with concomitant thyroid cancer. *Endocr Relat Cancer*. 2019;26(7):R395-R413.
2. Oka K, Yasuda M, Shien T, Otsuka F. A marked goiter involved in Marine-Lenhart syndrome. *J Gen Fam Med*. 2019;20(1):37-38.
3. Nishikawa M, Yoshimura M, Yoshikawa N, et al. Coexistence of an autonomously functioning thyroid nodule in a patient with Graves' disease: an unusual presentation of Marine-Lenhart syndrome. *Endocr J*. 1997;44(4):571-574.
4. Damle NA, Mishra R. Identifying Marine-Lenhart syndrome on a (99m)Tc-pertechnetate thyroid scan. *Indian J Endocrinol Metab*. 2013;17(2):366.
5. Joven MH, Anderson RJ. Marine-Lenhart syndrome. *Endocrine*. 2015;49(2):570-571.
6. Cakir M. Diagnosis of Marine-Lenhart syndrome. *Thyroid*. 2004;14(7):555.
7. Lombardi M, Tonacchera M, Macchia E. A new case of Marine-Lenhart syndrome with a papillary thyroid carcinoma. *Clin Case Rep*. 2018;6(12):2299-2302.
8. Uludag M, Aygun N, Ozel A, et al. A rare presentation of autonomously functioning papillary thyroid cancer: malignancy in Marine-Lenhart syndrome nodule. *Case Rep Surg*. 2016;2016:8740405.
9. Zhuang Y, Li C, Hua Z, Chen K, Lin JL. A novel TIRADS of US classification. *Biomed Eng Online*. 2018;17(1):82.
10. Mistry R, Hillyar C, Nibber A, Sooriyamoorthy T, Kumar N. Ultrasound classification of thyroid nodules: a systematic review. *Cureus*. 2020;12(3):e7239.

11. Feldkamp J, Führer D, Luster M, Musholt TJ, Spitzweg C, Schott M. Fine needle aspiration in the investigation of thyroid nodules. *Dtsch Arzteblatt Int.* 2016;113(20):353-359.
12. Waisman J. Thyroid fine-needle aspiration. *Am J Clin Pathol.* 2009;131(5):750.
13. Erkinuresin T, Demirci H. Diagnostic accuracy of fine needle aspiration cytology of thyroid nodules. *Diagn Berl Ger.* 2020;7(1):61-66.
14. Durante C, Hegedüs L, Czarniecka A, et al. 2023 European Thyroid Association clinical practice guidelines for thyroid nodule management. *Eur Thyroid J.* 2023;12(5):e230067.
15. Charkes ND. Graves' disease with functioning nodules (Marine-Lenhart syndrome). *J Nucl Med.* 1972;13(12):885-892.
16. Falch C, Axt S, Scuffi B, Koenigsrainer A, Kirschniak A, Muller S. Rapid thyroid nodule growth is not a marker for well-differentiated thyroid cancer. *World J Surg Oncol.* 2015;13(1):338.
17. Lau LW, Ghaznavi S, Frolkis AD, et al. Malignancy risk of hyperfunctioning thyroid nodules compared with non-toxic nodules: systematic review and a meta-analysis. *Thyroid Res.* 2021;14(1):3.
18. Scherer T, Wohlschlaeger-Krenn E, Bayerle-Eder M, et al. A case of simultaneous occurrence of Marine-Lenhart syndrome and a papillary thyroid microcarcinoma. *BMC Endocr Disord.* 2013;13(1):16.
19. Reschini E, Ferrari C, Castellani M, et al. The trapping-only nodules of the thyroid gland: prevalence study. *Thyroid.* 2006;16(8):757-762.
20. Integrated genomic characterization of papillary thyroid carcinoma. *Cell.* 2014;159(3):676-690.
21. Abdullah MI, Junit SM, Ng KL, Jayapalan JJ, Karikalan B, Hashim OH. Papillary thyroid cancer: genetic alterations and molecular biomarker investigations. *Int J Med Sci.* 2019;16(3):450-460.
22. Sharma A. Marine-Lenhart syndrome in two adolescents, including one with thyroid cancer: a case series and review of the literature. *J Pediatr Endocrinol Metab.* 2017;30(12):1237-1243.
23. Danno H, Nishihara E, Kousaka K, et al. Prevalence and treatment outcomes of Marine-Lenhart syndrome in Japan. *Eur Thyroid J.* 2021;10(6):461-467.
24. Hu L, Wu Y. Papillary thyroid carcinoma presenting as a functioning thyroid nodule: report of 2 rare cases. *Int J Clin Exp Pathol.* 2020;13(11):2895-2906.
25. Leboulleux S, Bournaud C, Chougnet CN, et al. Thyroidectomy without radioiodine in patients with low-risk thyroid cancer. *N Engl J Med.* 2022;386(10):923-932.